Understanding Pre-Attentive and Attentive Processing of Non-Linguistic and Linguistic Auditory Stimuli: A Simultaneous EEG/MEG Study

Talya Inbar

UNDERSTANDING PRE-ATTENTIVE AND ATTENTIVE PROCESSING OF NON-LINGUISTIC AND LINGUISTIC AUDITORY STIMULI: A SIMULTANEOUS EEG/MEG STUDY

by

Talya Inbar

A research thesis completed under the direction of
Dr. Mireille Besson and Dr. Valérie Chanoine

In collaboration with Dr. Jean-Michel Badier, Dr. Christian Bénar, Thomas Chehrerian, Marie Edet, Dr. Aline Frey, and Khoubeib Kanzari

Submitted in fulfillment of the requirements for the degree of

Master 2, Cognitive Science
Langage, Communication and the Brain

Aix-Marseille Université, UFR ALLSH

May 2023

Abstract

English

Based on research indicating the potential benefits of using simultaneous electroencephalography (EEG) and magnetoencephalography (MEG) recordings to examine sensor- and source-level neuronal activity, this study aimed to establish an experimental procedure to investigate pre-attentive and attentive processing of harmonic (non-linguistic) and syllable (linguistic) sounds using these two modalities. We analyzed results at the sensor-level, allowing us to compare event-related potentials (ERPs) and event-related fields (ERFs), and these results will soon be completed with source-level localizations. In doing so, we found important similarities between information captured by ERP and ERF data, as well as overall differences in the amplitude of pre-attentive and attentive components in response to auditory stimuli. These results thus contribute to a wide base of auditory attention literature, while also providing a comprehensive look at the similarities and differences between EEG and MEG in studying auditory processing.

Français

Sur la base de recherches indiquant les avantages potentiels de l'utilisation d'enregistrements simultanés d'électroencéphalographie (EEG) et de magnétoencéphalographie (MEG) pour étudier l'activité neuronale au niveau des capteurs et des sources, cette expérience visait à établir une procédure expérimentale pour analyser le traitement pré-attentif et attentif de sons harmoniques et de syllabes en utilisant ces deux modalités. Dans ce mémoire, nous avons traité nos résultats au niveau des capteurs, ce qui nous a permis de comparer les potentiels évoqués et les potentiels de champs. Ces résultats seront bientôt complétés par des analyses de localisation de sources. Nous avons constaté des similitudes importantes entre les informations fournies par les données ERP et ERF, ainsi que des différences globales dans l'amplitude des composantes pré-attentives et attentives associées aux stimuli auditifs. Ces résultats apportent de nouvelles informations à une littérature déjà importante sur l'attention auditive, tout en ajoutant des données précises sur les similitudes et les différences entre l'EEG et la MEG dans l'étude du traitement auditif.

Table of Contents

Introduction

Although electroencephalography (EEG) and magnetoencephalography (MEG) are two of the most ubiquitous techniques for studying human brain activity, their advantages and disadvantages for analyzing surface and source-level activity have yet to be fully understood. While MEG is traditionally considered to have better spatial resolution than EEG, these two methods are also complementary, as MEG detects neural currents from tangential sources and EEG detects both tangential and radial sources (Puce & Hämäläinen, 2017). The present study aimed to determine the extent of this complementarity and evaluate the differences between the two methods for studying pre-attentive and attentive processing. In doing so, it contributes to a wide body of auditory attention literature while also addressing an important methodological question by comparing EEG and MEG data at the level of electrodes and magnometer sensors and through source localization.

Attention can be defined as the allocation of resources towards relevant stimuli. This allocation can be automatic, in the case of pre-attentive processing, or deliberate, in the case of attentive processing. EEG and MEG, which allow for non-invasive recording and analysis of millisecond brain activities based on the electromagnetic fields generated by neural currents (Baillet, 2011), have both been used to investigate these processes. In EEG studies, the well-documented Mismatch Negativity (MMN) component is considered a signature of pre-attentive processing, as it is evoked in response to a change in auditory stimulation while participants are not paying attention to the stimuli (Näätänen, Gaillard, & Mäntysalo, 1978). Typically, MMNs are studied using a passive oddball protocol, where a standard sound stimulus is played several times, and then is infrequently interspersed with a different, deviant sound. The MMN is computed as the difference in measured brain activity associated with these standard and deviant auditory stimuli and is elicited primarily in frontal and temporal regions (Näätänen, Pakarinen, Rinne, & Takegata, 2004; Rinne, Alho, Ilmoniemi, Virtanen, & Näätänen, 2000). EEG studies using auditory stimuli have made use of the MMN to show that it can be elicited by a change in several sound properties, including frequency, intensity, and duration, thus indicating that these acoustic properties are automatically processed (Fitzgerald & Todd, 2020; Näätänen, 1992). MEG studies have used the MMN's magnetic equivalent (the MMNm) to study pre-attentive processing using melodies and vowel sounds to show that changes in stimulus contour (the pattern of pitch changes between notes in a sequence), interval, and phoneme category can all elicit MMNm responses (Fujioka, Trainor, Ross, Kakigi, & Pantev, 2004; Shestakova et al., 2002).

Meanwhile, at the level of attentive processing, the P300 component occurs when participants are actively listening to detect deviant stimuli and is thought to reflect neural mechanisms related to attention and memory updating (Donchin, 1981; Picton, 1992; Polich, 2007). The P300 can be broken down into P3a and P3b components, where the first is frontally located and is taken to reflect the automatic orientation of attention towards a surprising event and the second is parietally located and has been associated with the direction of attention towards relevant stimuli as well as decision making (Polich, 2003). Previous studies using EEG have shown that changes in both intensity and frequency of pure tone auditory stimuli evoke P300 responses (Osorio, Irani, Herrada, & Aboitiz, 2022; Sugg & Polich, 1995). However, the MEG equivalent, the P300m, is less documented, and previous investigations using auditory stimuli have shown little consistent MEG activity around the time of the P300 component (Siedenberg, Goodin, Aminoff, Rowley, & Roberts, 1996). Importantly, both the P300 and MMN components have shown variations in amplitude and latency depending on the magnitude of difference between standard and deviant stimuli, where the easier a deviant is to discriminate, the larger and earlier the MMN and P300 components are (Näätänen, 1992; Pakarinen, Takegata, Rinne, Huotilainen, & Näätänen, 2007; Picton, 1992). While well established in EEG studies, to our knowledge, this pattern has been less widely studied using MEG, and thus we are interested in making this comparison between EEG and MEG results at the sensor level.

To investigate the effects of attention on auditory processing, we presented participants with non-linguistic and linguistic auditory stimuli in both pre-attentive and attentive conditions. In the non-linguistic conditions, participants heard standard harmonic complex sounds as well as large, intermediate, and small deviant sounds, which varied from the standard sound in terms of frequency. At the sensor level, we compared Event-Related Potentials (ERPs) with Event-Related Fields (ERFs) to analyze our EEG and MEG data. We hypothesized that, in both the pre-attentive and attentive conditions, large deviant stimuli, which differed the most from the standard sound, would evoke MMN, MMNm, P3b, and P3bm components with larger amplitudes and shorter latencies than intermediate and small deviant stimuli. Such results would replicate previous findings in the literature for EEG data (Frey, Barbaroux, Dittinger, & Besson, 2022; Näätänen, Paavilainen, Rinne, & Alho, 2007; Picton, 1992) and thus the non-linguistic stimuli served as a control to validate our experimental design. Across all experimental conditions, our sensor level EEG and MEG hypotheses were the same, as previous studies have shown similar results when comparing ERPs and ERFs using passive and active auditory oddball protocols (Huotilainen et al., 1998; Korostenskaja, Kičić, & Kähkönen, 2008; Lecaignard, Bertrand, Caclin, & Mattout, 2021).

In the linguistic conditions, we presented monosyllabic Thai stimuli with the syllable /pa:1/ as the standard stimulus along with syllables that varied in voicing (/ba:1/), in aspiration (/p^ha:1/) and in pitch (/pa:0/) as the deviant stimuli. Considering that syllables are one of the building blocks of language, the syllable stimuli were of particular interest in this experiment to further understand how human brain activity reflects the analysis of basic linguistic information. We hypothesized that the voicing deviant stimulus, which belongs to the French phonetic repertoire, would be the easiest to discriminate for French-speaking participants and would thus evoke MMN, MMNm, P3b, and P3bm components with larger amplitudes and shorter latencies than both the aspiration and the pitch deviant syllables, which are unfamiliar phonetic contrasts and absent from the French repertoire. For both non-linguistic and linguistic stimuli, we expected these predicted deviant stimuli difficulty levels to be reflected through error percentages and reaction times in corresponding behavioral data.

Finally, we also intend to analyze our data at the source level by performing source localization for both EEG and MEG data. While this has not yet been completed, here I will discuss our goals for source localization as well as provide a general outline for how we plan to perform these analyses in the coming weeks. Source localization is of interest as it would directly respond to the traditional claim that MEG has better spatial resolution than EEG using simultaneously recorded data from the same subjects in identical experimental conditions. It also offers us the potential of investigating the similarities and differences in the brain regions involved during pre-attentive and attentive processing of two different types of auditory stimuli, harmonic sounds and syllables. At the pre-attentive level, one previous EEG study using a typical MMN protocol with tone stimuli identified the precentral gyrus as the location of maximum MMN intensity when data were analyzed using exact low resolution brain electromagnetic tomography (eLORETA) software (Takahashi et al., 2012). In another study using standard and deviant auditory tone stimuli, authors used high density EEG and individual magnetic resonance images to perform dipole source localization, with which they localized the MMN in the superior temporal gyri, notably Heschl's gyrus (Ha et al., 2003). This result has been widely replicated in MEG studies using a typical auditory MMN protocol (Hari, 1990; Huotilainen et al., 1998; Mäkelä, Hämäläinen, Hari, & McEvoy, 1994; Nakasato et al., 1994; Pantev et al., 1995; Reite et al., 1994; Rogers, Papanicolaou, Baumann, Saydjari, & Eisenberg, 1990).

At the attentive level, one EEG study using LORETA localized the P300 component to the prefrontal cortex, anterior and posterior cingulate cortex, and the temporal and parietal lobes (Winterer et al., 2001). Other studies, which compared the P3b and P3a components using an

active auditory oddball paradigm, found the P3a component to be more anteriorly located in the anterior superior temporal gyrus (Alho et al., 2001), the prefrontal cortex (He, Lian, Spencer, Dien, & Donchin, 2001) and the anterior cingulate (Dien, Spencer, & Donchin, 2003**;** for review see Linden, 2005) than the P3b component. Several MEG studies have localized the auditory P300m to the medial temporal and superior temporal regions (Tarkka, Stokic, Basile, & Papanicolaou, 1995; Nishitani, Nagamine, Fujiwara, Yazawa, & Shibasaki, 1998; Gordon et al., 1987) and to inferior parietal regions (Nishitani, Nagamine, Fujiwara, Yazawa, & Shibasaki, 1998). Another study, using a single-dipole model and an active auditory oddball design found P300 activity recorded using both EEG and MEG to start at deep sources and then spread across the auditory cortex (Rogers, 1991). The benefits of simultaneous EEG and MEG recording for source localization have been reported by Sharon et al. (2007), where authors cited the complementary nature of these two modalities. Here, we hope to better understand and take advantage of this complementarity in the context of pre-attentive and attentive auditory processing. Overall, as activated sources depend on the type of stimuli that provoke ERP and ERF responses, we expect to see differences in source localization for HCS and SYL stimuli and are also interested in comparing these results between attention conditions and modalities.

Our study serves as a continuation of a pilot study performed in 2022, where we were familiarized with the technical aspects of combined EEG and MEG recordings and validated our procedure and stimuli for continued use. Here, I will present the majority of our data and analyses, which are done at several levels. First, comparing pre-attentive and attentive auditory processing using the same stimuli, and second doing this within the scope of both EEG and MEG signals and comparing these signals at sensor and source levels. While I will present sensor-level analyses for both EEG and MEG data here, as mentioned above, the complexity of this project as well as time constraints meant we were not able to finalize our source-level analyses for this master's thesis. Nevertheless, I will provide an outline of how this will be performed, and I will continue working on these analyses through the month of June.

Materials and Methods

Participants

The participants in this study were 21 adults (15 women and 6 men) ranging from 19 to 27 years old. Of these participants, 7 were excluded from the harmonic complex sounds condition (thus N= 14) and two were excluded from the syllables condition (thus N= 19) due either to time constraints or to a low signal-to-noise ratio in EEG data. Inclusion criteria were the absence of neurological disorders, native fluency in a non-tonal language, and meeting MEG safety standards. Participants provided written consent to participate in the study and

were compensated for their time at a rate of 12 euros per hour. The study was performed in accordance with Aix-Marseille University's "Committee for the Protection of Individuals" standards (CPP 2017-A03614–49).

Stimuli

Two categories of auditory stimuli were presented: harmonic complex sounds (HCS) and syllables (SYL). All HCS were equated for duration (237 ms) and intensity (60 dB) and were varied in pitch to create a standard stimulus (195 Hz) as well as large (235 Hz; 40 Hz difference), intermediate (215 Hz; 20 Hz difference), and small (200 Hz; 5 Hz difference) deviant stimuli. These stimuli have previously been shown to elicit a reliable MMN response (Frey, Barbaroux, Dittinger, & Besson, 2022). SYL stimuli were Thaï syllables with an average duration of 530 ms that were also equated for intensity (60 dB). The standard stimulus was /pa:1/, with a voice onset time (VOT) of 3 ms and a fundamental frequency (*f0*) of 175 Hz. Three deviant stimuli, which varied in voicing: /ba:1/ (VOT = -144 ms), aspiration: p^ha:1/ (VOT = 77 ms), and pitch: /pa:0/ (*f0* = 218 Hz) were also used.

Procedure

Throughout the experiment, participants were individually tested while lying down on a MEG bed in a Faraday cage. Auditory stimuli were delivered binaurally through plastic tubes terminating in MEG-compatible earbuds at a volume deemed comfortable by participants at the start of each experimental block. Stimuli were presented using Presentation software (Neurobehavioral Systems, Berkley, CA; neurobs.com/).

Experimental Design

This experiment was organized into a pre-attentive and an attentive block, where both types of stimuli (HCS or SYL) were presented in each block, resulting in four experimental conditions (Figure 1). In the pre-attentive conditions, participants watched a self-selected silent movie while HCS or SYL were played through earbuds. They were instructed not to pay attention to auditory stimuli and to focus their attention on the movie. In the attentive conditions, participants heard the same stimuli as in the pre-attentive conditions but were no longer presented with a movie. Instead, participants were asked to focus their attention on the HCS or SYL and to press a response button each time they heard a deviant stimulus. The pre-attentive block was always performed first and the attentive block second, and the order of presentation for the type of stimulus was balanced across participants. A total of 1,214 stimuli were presented within each experimental condition, with 854 repetitions of the standard sound (including 14 at the start to establish a short-term memory trace) and 120 repetitions of each deviant sound. Stimulus presentation was organized such that at least one and at most four

standard stimuli were presented in between two deviant stimuli, with no more than three deviant stimuli presented in a row. For HCS stimuli, stimulus-onset-asynchrony was 600 ms, while for

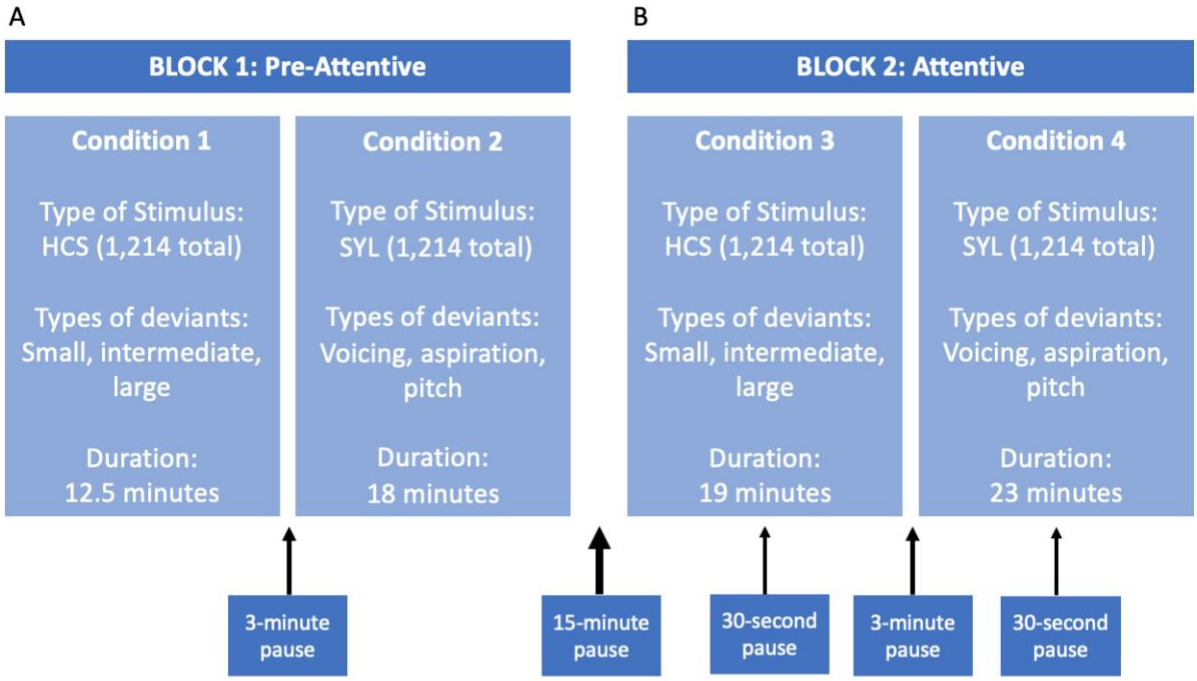

Figure 1. Example of an experimental setup for one participant. Participants were presented with auditory stimuli in two blocks. In this example setup, the participant was presented first with HCS stimuli and then SYL stimuli in the pre-attentive block (A) and attentive block (B). The order of the type of stimulus presented within each block was balanced across participants, such that half of the participants had the experimental setup shown here, and the others heard SYL stimuli before HCS stimuli in each block. Five pauses of varying durations were included throughout the experiment.

SYL stimuli, it was 800 ms. Consequently, the duration of the pre-attentive HCS condition was 12.5 minutes and the duration of the pre-attentive SYL condition was 18 minutes. The attentive conditions were slightly longer to allow for participant response time, with a 19-minute duration for the attentive HCS condition and a 23-minute duration for the attentive SYL condition. A 30-second pause was included in the middle of each attentive condition to promote participant attentiveness. Each experimental condition was separated by a pause of about 3 minutes to allow the MEG machinery to reset, while a longer pause of about 15 minutes was included between the two blocks to maintain participant comfort.

Neurophysiological Recording

EEG and MEG were recorded simultaneously from 64 EEG electrodes (Ag/AgCl EEG cap, Brain Products amplifier) and 248 magnetometers (4D whole head Neuroimaging system WH3600TM) with a sampling rate of 2,500 Hz. For EEG recording, conductive gel was injected into each electrode to improve contact between the electrode and the scalp. Electrode impedance was kept below 10 kΩ, with most impedances below 5 kΩ. A vertical electrooculogram (EOG) was recorded from flat-type active electrodes positioned just above and below the left eye. The electrocardiogram (ECG) was recorded from two additional electrodes, one placed on the upper left side of the chest, and one placed on the lower right

abdomen. Five coils were fixed on each participant's electrode cap to determine the position of the head relative to the MEG captors. These coils, the head shape, and the electrodes were digitized using a 3-D digitizer (Polhemus Fastrack, Polhemus Corporation, Colchester, VT), which allowed the head position to be recorded before and after each experimental condition.

Data Analysis

All EEG and MEG data were analyzed and visualized in Python (Version 3.10.4) using MNE Software (Version 1.3.1; Larson et al., 2023) and the MNE-Python package (Gramfort et al., 2013).

Pre-processing of EEG and MEG Data

Following simultaneous recordings, EEG and MEG signals were synchronized based on stimulus triggers and combined into one file using AnyWave (Colombet, Woodman, Badier, & Bénar, 2015). EEG and MEG data were then pre-processed simultaneously using MNE-Python. First, EEG and MEG channels were renamed to align with MNE-Python formatting. EEG data were then re-referenced offline to the average of all channels (excluding EOG and ECG channels). Next, EEG and MEG data were IIR filtered using a low-frequency cutoff of 0.1 Hz and a high-frequency cutoff of 30 Hz, and resampled to 500 Hz, as the original higher frequency was needed to correctly synchronize files but was not necessary for our analyses. Finally, system artifact rejection was performed visually on the basis of the power spectrum density. Physiological artifacts were then detected and removed using a signal space projection.

Behavioral Analysis

Once data were pre-processed, response data from the attentive blocks were analyzed for HCS and SYL stimuli. Responses within each condition were grouped according to the type of deviant: large, intermediate, and small for HCS or voicing, pitch and aspiration for SYL. Then, for each type of deviant, percent error and response time were calculated.

Sensor-Level Analysis: ERPs and ERFs

In order to visualize Event-Related Potentials (ERPs) and Event-Related Fields (ERFs), pre-processed combined EEG and MEG files were read using MNE-Python. EEG and MEG data were then segmented into epochs beginning 100 ms before and ending 800 ms after stimulus presentation. Next, an additional artifact rejection was performed on each trial to exclude electrode amplitudes above 75 µV and magnometer amplitudes above 5e-12 T. A baseline correction was then applied in the time frame of 100 ms before stimulus onset, where activity was averaged and set to zero. Activity recorded after stimulus presentation was computed relative to this baseline. In the attentive block, trials in which participants responded incorrectly were excluded. Finally, for each participant, epochs were averaged and time-locked

to stimulus presentation for each experimental condition and for each deviant type. These averaged combined EEG and MEG files were then used to compute the grand averages across participants as well as for statistical analyses. To visualize ERPs and ERFs, the average signal from each deviant type was subtracted from that of the standard to create a difference wave. Although difference waves are typically used to present only MMNs, here we used them for both the MMN and P300 components, as this allowed for easier visualization and comparison across experimental conditions. Grand average difference waves were calculated and plotted according to 9 regions of interest (ROIs), where signal data was averaged across the sensors in each ROI. The ROIs were organized as follows: frontal left, central left, parietal left, frontal midline, central midline, parietal midline, frontal right, central right, and parietal right. For a full list of sensors included in each ROI, see Appendix B.

Source-Level Analysis

Although our source-level analysis has not yet been completed, it is the next step in our study, and we have begun to determine the methods by which we will perform these analyses. Here, I will present an overview of these methods, to be carried out during the month of June.

In order to perform source-level analysis on our EEG and MEG data, we will need both source and head models. For our source model, we will use an MRI template that has been standardized and has brain ROIs labeled. Ideally, these ROIs would be volumetric, and would be based on a brain atlas to determine ROI locations. The head model, which will allow us to determine how currents circulate and flow from sources to EEG and MEG captors, will depend both on head geometry as well as tissue conductivity. For this, we will use the digitization information gathered for each participant, providing us with head shape data that we will use to deform our head model, affecting both the head and the sources. Finally, we will likely apply a minimum norm algorithm to determine the time-course of EEG and MEG data, which we can then group into ROI clusters to use for statistical analyses to determine source locations from each set of data.

Statistical Analysis

Statistical analysis was performed in Python (Version 3.10.4) using the Statsmodels module (Seabold & Perktold, 2010). Repeated measures analyses of variance (ANOVAs) were used to analyze behavioral, EEG, and MEG data.

For behavioral data, ANOVAs with type of deviant as the factor were performed for percentage of error and reaction time for both HCS and SYL stimuli. Tukey tests were then used for post hoc comparisons.

For sensor-level analyses, ERPs and ERFs were separated into time windows that best captured MMN and P300 components. In this paper, I will report results from a subset of these time windows, where the most relevant activity was seen. For pre-attentive conditions with HCS stimuli, and as can be seen on Figures 3 and 4, large deviants were associated with both an early and a late MMN or MMNm, while intermediate and small deviants were only associated with a late MMN or MMNm. These effects were captured in the 100-190 ms and 260-420 ms latency bands, respectively. For attentive conditions with HCS stimuli, effects were tested from 70-200 ms, for early positivities, and 200-550 ms, for P3b and P3bm components. For pre-attentive conditions with SYL stimuli, effects were tested in two latency bands: 140-300 ms and 300-450 ms, again to capture early and late MMN and MMNm components. Finally, for attentive conditions with SYL stimuli, effects were tested from 100-250 ms, again for early positivities, and from 250-500 ms, for P3b and P3bm components. ANOVAs performed within these time windows included type of deviant and ROIs as factors. For pre-attentive conditions, the dependent variables measured were negative peak (MMN/MMNm) amplitude and latency, whereas for attentive conditions they were positive peak (P3b/P3bm) amplitude and latency. Due to time constraints, the post-hoc test results for sensor-level data will not be included here, although these analyses are in progress and will be completed in the coming weeks.

Results

Here, I will present results from behavioral data as well as sensor-level analyses (ERPs and ERFs) across all conditions and for both EEG and MEG data. These results are preliminary, as we have not yet completed the full scope of additional analyses we plan to perform to verify our results. Nevertheless, they indicate important patterns in terms of stimulus deviant difficulty as well as similarities and differences between both EEG and MEG modalities and pre-attentive and attentive processing.

Harmonic Complex Sound Stimuli

Behavioral Data

Results from the attentive task showed that for HCS stimuli, the main effect of deviance was not significant for the percentage of error (Figure 2A). However, it was significant for reaction times ($F_{2,26}$ = 50.79, p < .001), with significantly shorter reaction times for large deviant stimuli than intermediate (p < .001) or small (p < .001) deviant stimuli, as well as shorter reaction times for intermediate than small deviant stimuli (p = .036; Figure 2B).

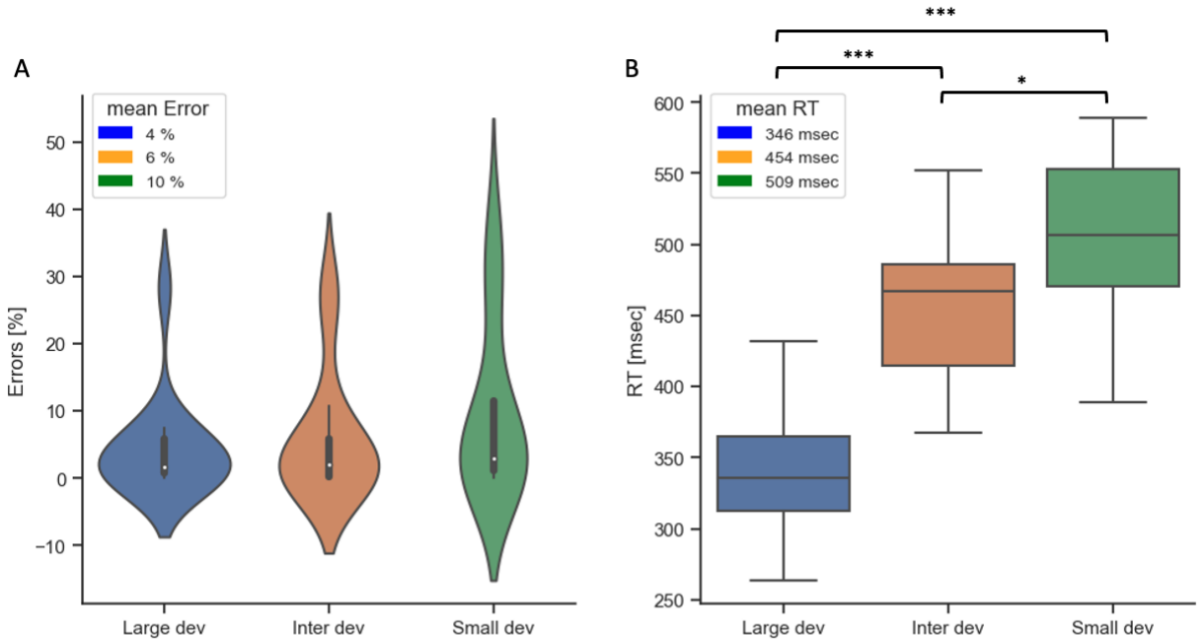

Figure 2. Behavioral results from the attentive HCS condition show no change in percent error but an increase in reaction time from large to intermediate to small deviant stimuli. Percent error (A) and reaction times (B) were averaged across fourteen participants. Significance from post hoc Tukey tests are reported on the figure, where * = $p < .05$, ** = $p < .01$, *** = $p < .001$.

Pre-attentive Processing (MMN, MMNm): ERPs and ERFs

Regarding ERPs, for MMN amplitude in the HCS condition (Figure 3), both the main effect of deviance and the deviance-by-ROI interaction were significant in the time window of the early MMN from 100-190 ms (deviance: $F_{2,26} = 12.95$, $p < .001$; interaction: $F_{16,208} = 3.87$, $p < .001$), where MMN peak amplitude was the greatest for large deviant stimuli (-1.14 µV), followed by intermediate (-0.66 µV), and small (-0.62 µV) deviant stimuli. In the time window of the late MMN (260-420 ms), both the main effect of deviance and the deviance-by-ROI interaction were again significant (deviance: $F_{2,26} = 3.70$, $p = .038$; interaction: $F_{16,208} = 2.58$, $p = .001$), and MMN peak amplitudes were largest for large deviant stimuli (-1.09 µV), followed by small (-1.02 µV), and intermediate (-0.90 µV) deviant stimuli. For MMN peak latencies in both time windows, neither the main effect of deviance nor the deviance-by-ROI interaction was significant.

For corresponding ERFs, the early MMNm peak amplitude in the HCS condition (Figure 4) showed a significant main effect of deviance and deviance-by-ROI interaction (100-190 ms; deviance: $F_{2,26} = 8.32$, $p = .002$; interaction: $F_{16,208} = 8.20$, $p < .001$), where large deviant stimuli had the greatest negative peak amplitude (-35.0 fT), followed by small (-23.4 fT), and intermediate (-21.0 fT) deviant stimuli. Also in this time window, the MMNm peak latency had a significant main effect of deviance ($F_{2,26} = 4.55$, $p = .020$), where the intermediate deviant peak occurred the earliest (118 ms), followed by the large deviant (120 ms) and then

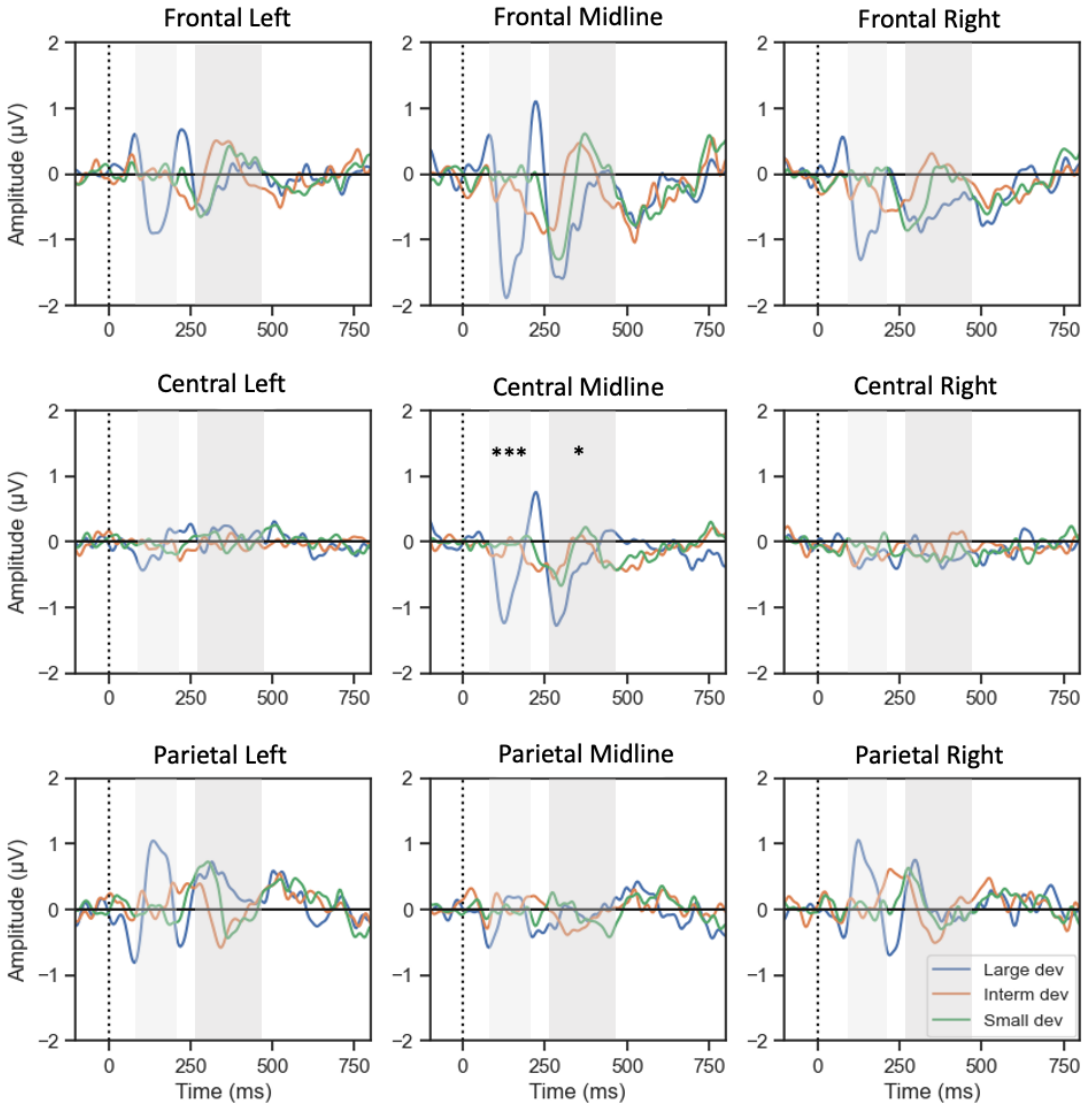

Figure 3. Pre-attentive ERPs for HCS stimuli across 9 ROIs show larger MMNs for large deviant stimuli than intermediate and small. ERPs were analyzed within two time windows: 100-190 ms (to capture the large deviant early MMN) and 260-420 ms (to capture large deviant late MMN and small and intermediate deviant MMNs). Because post-hocs have yet to be completed, significance values reported here are for the main effect of deviance (amplitude in black, latency, when applicable, in red), and are plotted on the central midline ROI (* = $p < .05$, ** = $p < .01$, *** = $p < .001$). Negative values are plotted downwards.

the small deviant (141 ms). The deviance-by-ROI interaction was not significant for MMNm peak latency in this time window. For the late MMNm peak amplitude (260-420 ms), the main effect of deviance was not significant, but the deviance-by-ROI interaction was ($F_{16,208} = 2.41$, $p = .003$). The deviance-by-ROI interaction was also significant for MMNm peak latency in this time window ($F_{16,208} = 2.32$, $p = .004$).

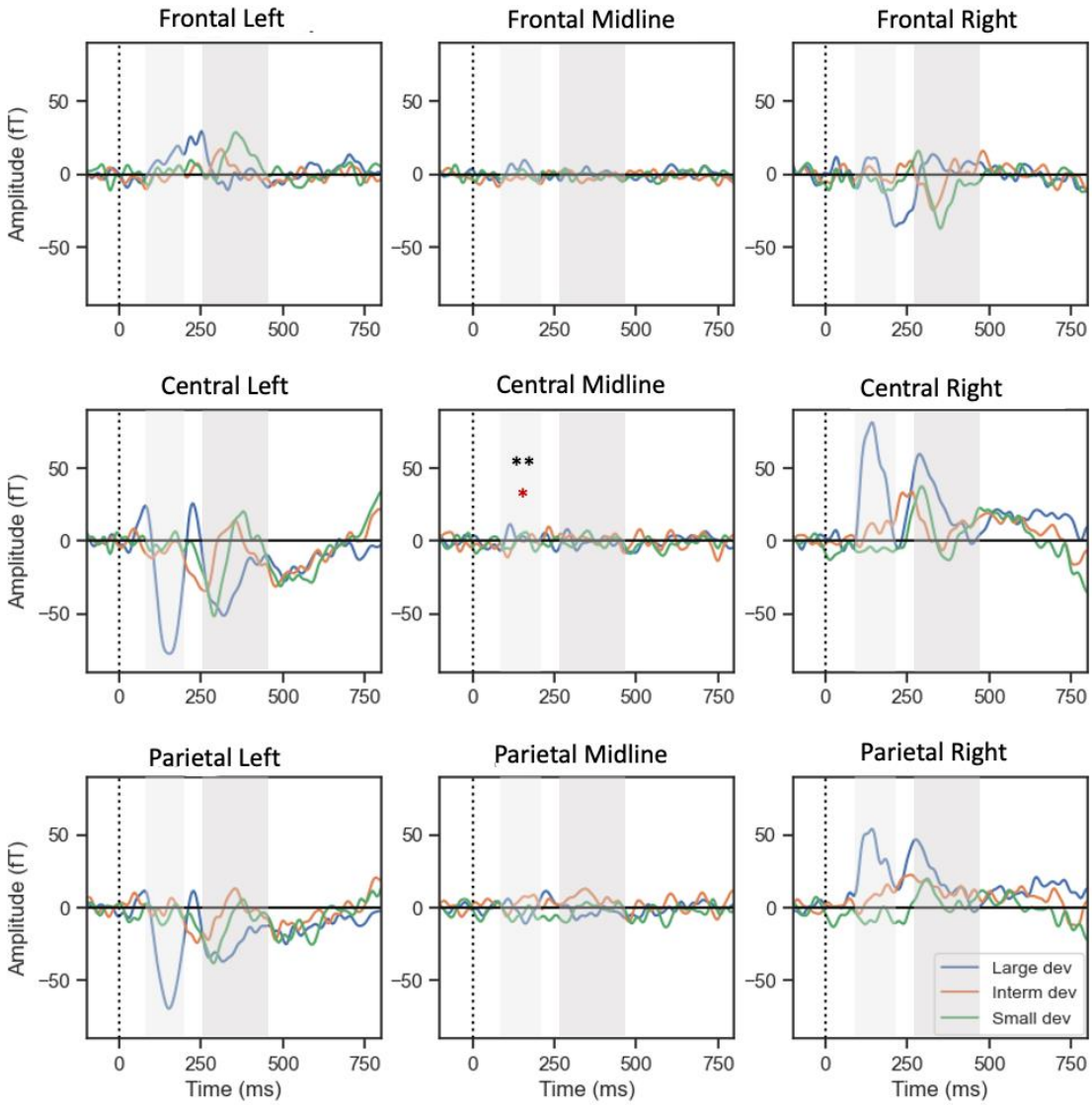

Figure 4. Pre-attentive ERFs for HCS stimuli across 9 ROIs show earlier and larger effects for large deviant stimuli than intermediate and small. ERFs were analyzed within two time windows: 100-190 ms (to capture the large deviant early MMNm) and 260-420 ms (to capture large deviant late MMNm and small and intermediate deviant MMNms). Because post-hocs have yet to be completed, significance values reported here are for the main effect of deviance (amplitude in black, latency, when applicable, in red), and are plotted on the central midline ROI (* = $p < .05$, ** = $p < .01$, *** = $p < .001$). Negative values are plotted downwards.

Attentive Processing (P3b, P3bm): ERPs and ERFs

For ERPs in the HCS condition (Figure 5), and for positive peak amplitude, both the main effect of deviance and the deviance-by-ROI interaction were significant in the early 70-200 ms time window (deviance: $F_{2,26} = 18.69$, $p < .001$; interaction: $F_{16,208} = 3.94$, $p < .001$), where the large deviant stimuli had the greatest positive peak amplitude (1.28 µV), followed by the small (0.76 µV), and intermediate (0.70 µV) deviant stimuli. In this same time window, both the main effect of deviance and the deviance-by-ROI interaction were significant for the latency of the positivity (deviance: $F_{2,26} = 7.42$, $p = .003$; interaction: $F_{16,208} = 2.79$, $p < .001$), where the small deviant peak occurred the earliest (90 ms), followed by the intermediate deviant

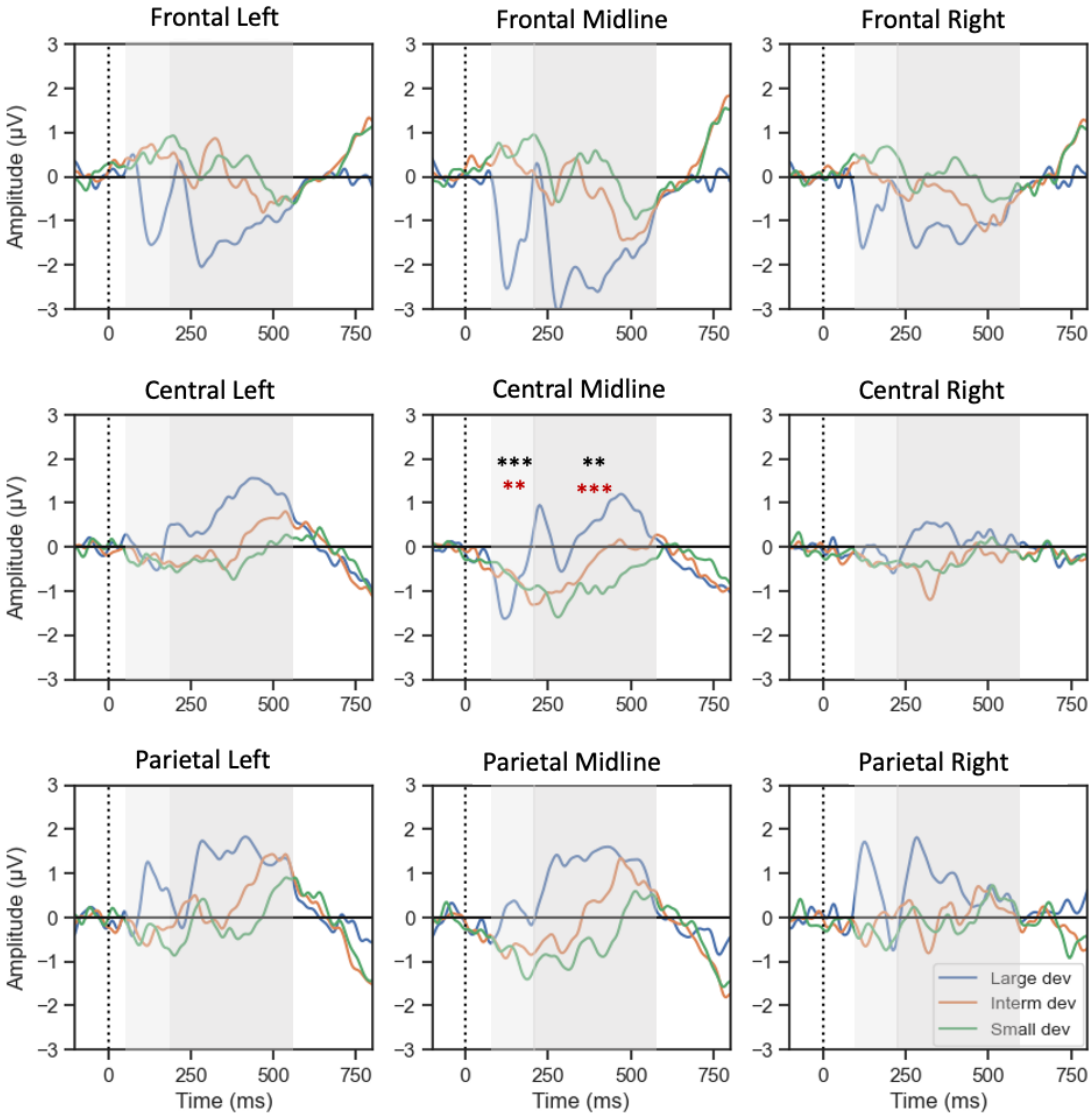

Figure 5. Attentive ERPs for HCS stimuli across 9 ROIs show earlier and larger P3bs for large deviant stimuli than intermediate and small. ERPs were analyzed within two time windows: 70-200 ms and 200-550 ms. Because post-hocs have yet to be completed, significance values reported here are for the main effect of deviance (amplitude in black, latency, when applicable, in red), and are plotted on the central midline ROI (* = $p < .05$, ** = $p < .01$, *** = $p < .001$). Negative values are plotted downwards.

(98 ms), and large deviant (120 ms). From 200-550 ms, the P3b amplitude showed a significant main effect of deviance and deviance-by-ROI interaction (deviance: $F_{2,26} = 7.74$, $p = .002$; interaction: $F_{16,208} = 2.75$, $p < .001$). Here, the P3b peak was the largest for large deviant stimuli (1.97 μV), followed by the intermediate (1.36 μV), and small (1.32 μV) deviant stimuli. The main effect of deviance, but not the deviance-by-ROI interaction, was significant for the P3b peak latency in this time window ($F_{2,26} = 16.58$, $p = .001$), which was the earliest for large deviant stimuli (297 ms), followed by small (344 ms), and intermediate (383 ms) deviant stimuli.

For ERFs in the HCS condition (Figure 6), and for positive peak amplitude, both the main effect of deviance and the deviance-by-ROI interaction were significant in the 70-200 ms

time window (deviance: $F_{2,26}$ = 14.12, p < .001; interaction: $F_{16,208}$ = 2.20, p = .006), where large deviant stimuli had the largest peak amplitude (54.9 fT), followed by intermediate (28.2 fT), and small (26.8 fT) deviant stimuli. Neither the main effect of deviance nor the deviance-by-ROI interaction was significant for the latency of the positivity in this time window. For

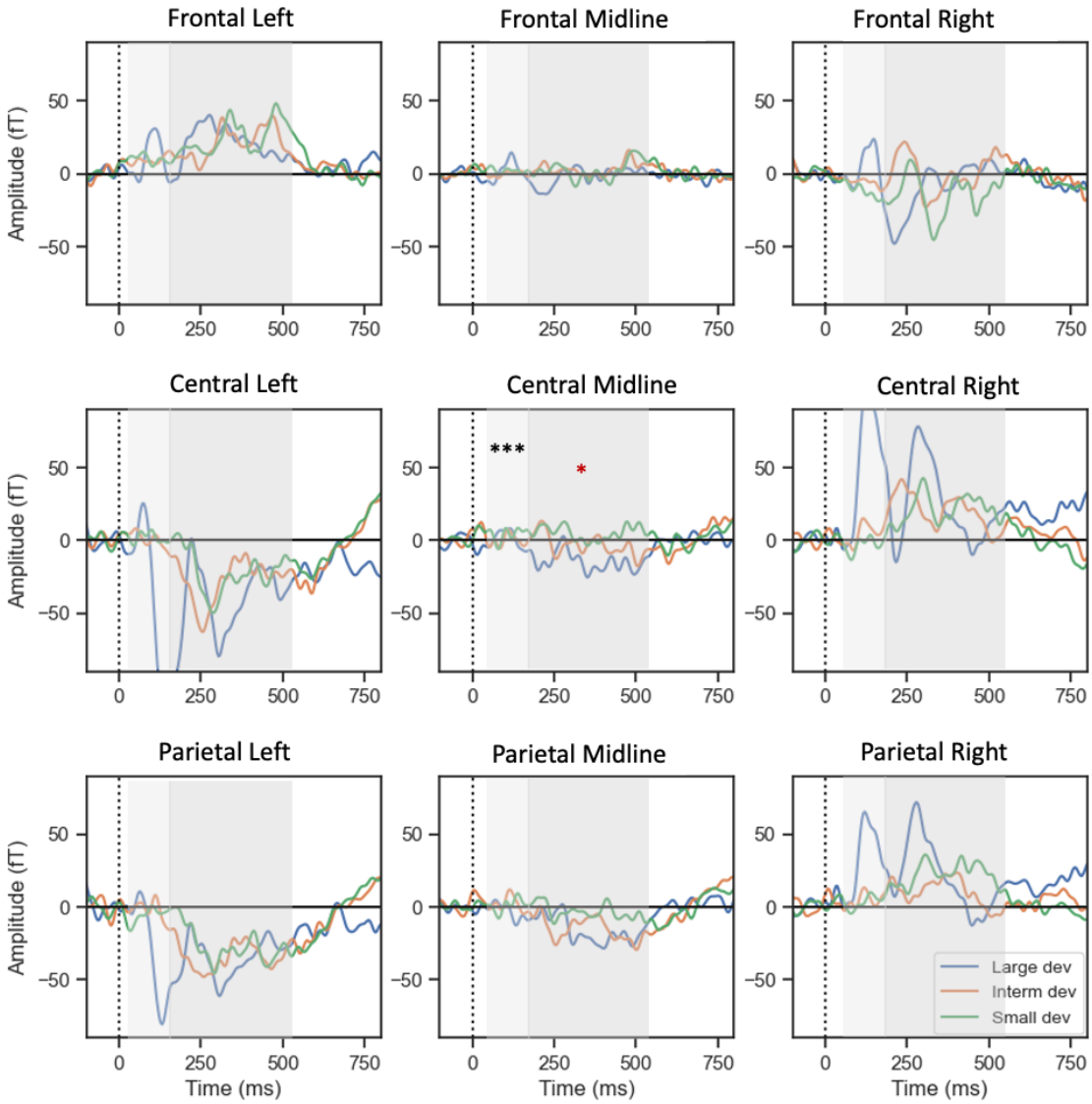

Figure 6. Attentive ERFs for HCS stimuli across 9 ROIs show earlier and larger effects for large deviant stimuli than intermediate and small. ERFs were analyzed within two time windows: 70-200 ms and 200-550 ms. Because post-hocs have yet to be completed, significance values reported here are for the main effect of deviance (amplitude in black, latency, when applicable, in red), and are plotted on the central midline ROI (* = p < .05, ** = p < .01, *** = p < .001). Negative values are plotted downwards.

P3bm peak amplitude from 200-550 ms, neither the main effect of deviance nor the deviance-by-ROI interaction was significant. However, both were significant for P3bm peak latency in this time window (deviance: $F_{2,26}$ = 5.14, p = .013; interaction: $F_{16,208}$ = 2.21, p = .006), where the large deviant peak was the earliest (281 ms), followed by the intermediate deviant (318 ms), and the small deviant (341 ms).

Syllable Stimuli

Behavioral Data

Results from the attentive task showed that for SYL stimuli, the main effect of deviance was not significant for the percentage of error made (Figure 7A). However, it was significant for reaction times ($F_{2,36}$ = 152.29, p < .001), where reaction times were longer for voicing deviant stimuli than pitch (p < .001) or aspiration (p = .004) deviant stimuli (Figure 7B).

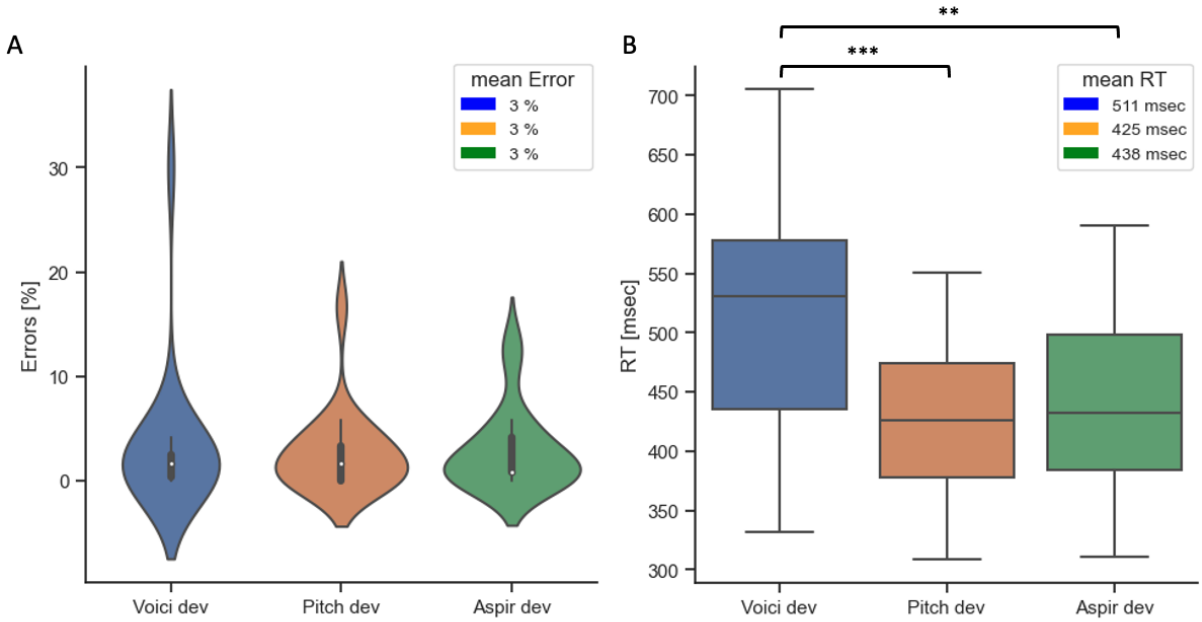

Figure 7. Behavioral results from the attentive SYL condition show a consistent percent error and an increase reaction time for voicing deviant stimuli. Percent error (A) and reaction times (B) were averaged across nineteen participants. Significance from post hoc Tukey tests are reported on the figure, where * = p < .05, ** = p < .01, *** = p < .001.

Pre-attentive Processing (MMN, MMNm): ERPs and ERFs

Regarding ERPs in the SYL condition, and for MMN peak amplitude in the 140-300 ms time window, both the main effect of deviance and the deviance-by-ROI interaction were significant (deviance: $F_{2,36}$ = 5.44, p = .009; interaction: $F_{16,288}$ = 3.98, p < .001), where aspiration deviant stimuli had the largest peak (-1.36 µV), followed by voicing (-1.02 µV), and then pitch (-0.93 µV) deviant stimuli (Figure 8). In the same time window for MMN peak latency, only the deviance-by-ROI interaction was significant ($F_{16,288}$ = 2.11, p = .008). Similarly, for MMN peak amplitude from 300-450 ms, only the deviance-by-ROI interaction was significant ($F_{16,288}$ = 13.18, p < .001). For MMN peak latency in this time window, both the main effect of deviance and the deviance-by-ROI interaction were significant (deviance: $F_{2,36}$ = 3.47, p = .042; interaction: $F_{16,288}$ = 4.38, p < .001). Voicing deviant stimuli peaked the earliest (283 ms), followed by aspiration (312 ms), and pitch (325 ms) deviant stimuli.

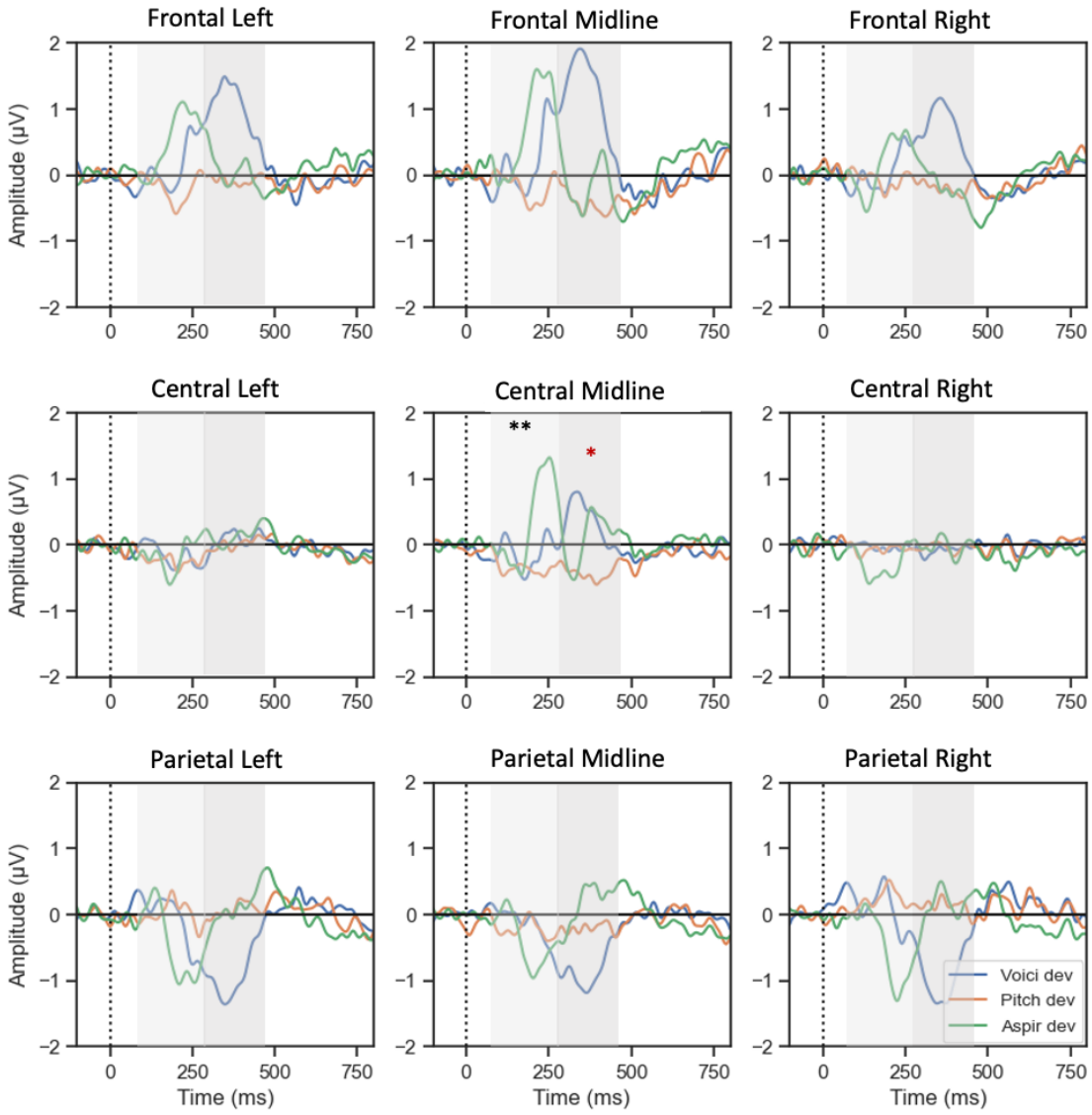

Figure 8. Pre-attentive ERPs for SYL stimuli across 9 ROIs show earlier and larger negativities for aspiration deviant stimuli than voicing and pitch. ERPs were analyzed within two time windows: 140-300 ms and 300-450 ms. Because post-hocs have yet to be completed, significance values reported here are for the main effect of deviance (amplitude in black, latency, when applicable, in red), and are plotted on the central midline ROI (* = $p < .05$, ** = $p < .01$, *** = $p < .001$). Negative values are plotted downwards.

For ERFs in the SYL condition, MMNm peak amplitude in the 140-300 ms time window had a main effect of deviance that was not significant, but a deviance-by-ROI interaction that was ($F_{16,288} = 4.00$, $p < .001$). MMNm peak latency in the same time window also showed only a deviance-by-ROI interaction that was significant ($F_{16,288} = 1.97$, $p = .020$). For MMNm peak amplitude and latency from 300-450 ms, the main effects of deviance and the deviance-by-ROI interactions were significant (amplitude deviance: $F_{2,36} = 3.99$, $p = .027$; amplitude interaction: $F_{16,288} = 8.45$, $p < .001$; latency deviance: $F_{2,36} = 7.63$, $p = .002$; latency interaction: $F_{16,288} = 3.66$, $p < .001$). The aspiration deviant stimuli had the largest MMNm peak (-32.0 fT), followed by voicing (-29.6 fT), and pitch (-25.6 fT) deviant stimuli (Figure 9).

Meanwhile, the voicing deviant stimuli peaked the earliest (306 ms), followed by pitch (351 ms), and then aspiration (355 ms) deviant stimuli.

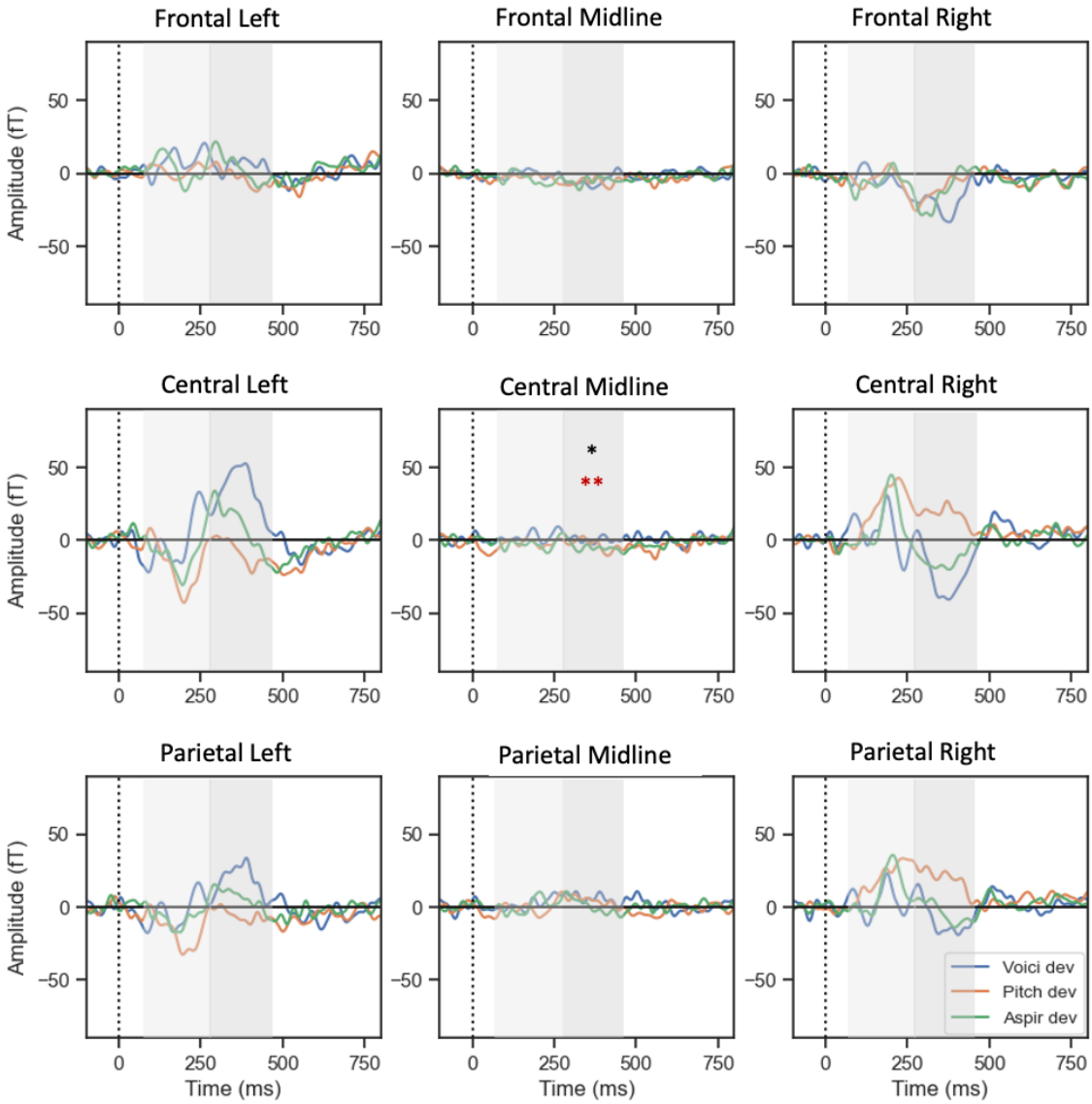

Figure 9. Pre-attentive ERFs for SYL stimuli across 9 ROIs show larger negativities for aspiration deviant stimuli than voicing and pitch. ERFs were analyzed within two time windows: 140-300 ms and 300-450 ms. Because post-hocs have yet to be completed, significance values reported here are for the main effect of deviance (amplitude in black, latency, when applicable, in red), and are plotted on the central midline ROI (* = $p < .05$, ** = $p < .01$, *** = $p < .001$). Negative values are plotted downwards.

Attentive Processing (P3b, P3bm): ERPs and ERFs

Regarding SYL ERPs (Figure 10), and specifically positive peak amplitude and latency from 100-250 ms, the main effects of deviance and the deviance-by-ROI interactions were significant (amplitude deviance: $F_{2,36} = 6.07$, $p = .005$; amplitude interaction: $F_{16,288} = 6.57$, $p < .001$; latency deviance: $F_{2,36} = 6.47$, $p = .004$; latency interaction: $F_{16,288} = 5.79$, $p < .001$). Aspiration deviant stimuli had the largest amplitude (1.34 µV), followed by voicing (1.09 µV), and pitch (0.85 µV) deviant stimuli. Meanwhile, voicing deviant stimuli peaked the earliest

(133 ms), followed by pitch (142 ms), and then aspiration (165 ms) deviant stimuli. For P3b peak amplitude from 250-500 ms, both the main effect of deviance and the deviance-by-ROI interaction were significant (deviance: $F_{2,36} = 5.53$, $p = .008$; interaction: $F_{16,288} = 3.75$, $p < .001$). Aspiration deviant stimuli had the largest amplitude (1.96 µV), followed by voicing (1.85 µV), and then pitch (1.49 µV) deviant stimuli. For P3b peak latency in this time window, only the main effect of deviance was significant ($F_{2,36} = 6.88$, $p = .003$). Aspiration deviant stimuli peaked the earliest (316 ms), followed by pitch (319 ms), and voicing (350 ms) deviant stimuli.

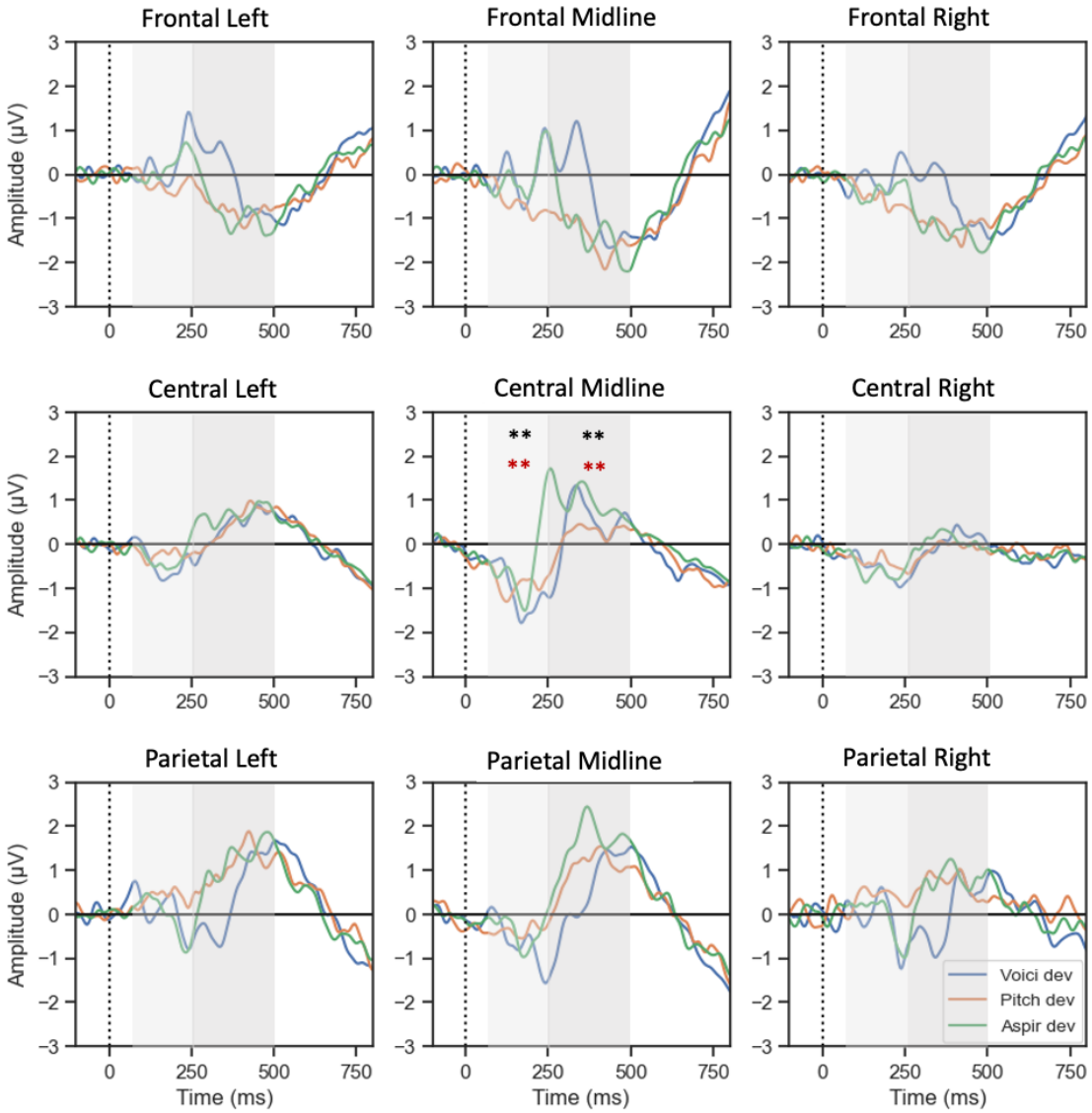

Figure 10. Attentive ERPs for SYL stimuli across 9 ROIs show earlier and larger P3bs for aspiration deviant stimuli than voicing and pitch. ERPs were analyzed within two time windows: 100-250 ms and 250-500 ms. Because post-hocs have yet to be completed, significance values reported here are for the main effect of deviance (amplitude in black, latency, when applicable, in red), and are plotted on the central midline ROI (* = $p < .05$, ** = $p < .01$, *** = $p < .001$). Negative values are plotted downwards.

For SYL ERFs (Figure 11), positive peak amplitude data from 100-250 ms had a significant main effect of deviance ($F_{2,36} = 6.55$, $p = .004$), but no significant deviance-by-ROI interaction. Aspiration deviant stimuli had the largest peak amplitude (54.5 fT), followed by

the voicing deviant (48.2 fT), and the pitch deviant stimuli (38.9 fT). From 250-500 ms, for P3bm peak amplitude, there was no significant main effect of deviance, but there was a significant deviance-by-ROI interaction ($F_{16,288}$ = 2.82, p < .001). Neither time window had significant main effects of deviance or deviance-by-ROI interactions for P3bm peak latency.

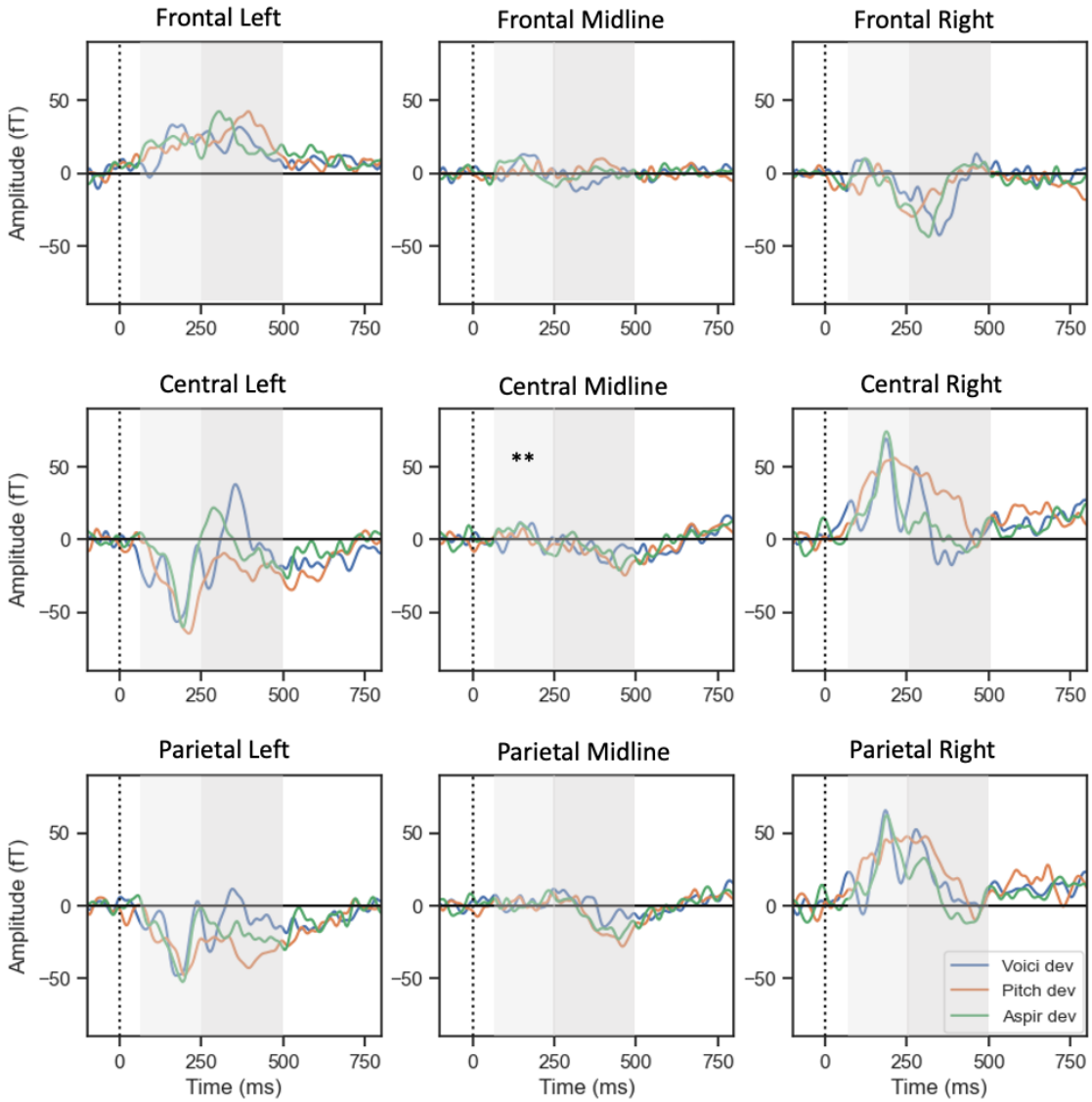

Figure 11. Attentive ERFs for SYL stimuli across 9 ROIs show larger positivities for aspiration deviant stimuli than voicing and pitch. ERFs were analyzed within two time windows: 100-250 ms and 250-500 ms. Because post-hocs have yet to be completed, significance values reported here are for the main effect of deviance (amplitude in black, latency, when applicable, in red), and are plotted on the central midline ROI (* = p < .05, ** = p < .01, *** = p < .001). Negative values are plotted downwards.

Discussion

Our goals for this study were to examine the processing of non-linguistic and linguistic auditory stimuli, and to compare the effects seen across attention conditions and modalities. Here, we have successfully met these goals at the level of electrodes and magnometer sensors, except for certain post-hoc tests and additional ANOVAs that will be performed to complement the results discussed in this master's thesis. Overall, results showed that the large deviant HCS

stimuli elicited larger MMN and MMNm, P3b, and P3bm components than intermediate and small deviant stimuli, which aligned with reaction time behavioral results. For SYL stimuli, ERPs and ERFs indicated that aspiration deviant stimuli were associated with larger MMN, MMNm, P3b, and P3bm components than voicing and pitch deviant stimuli, which also aligned with reaction time behavioral results. Across all conditions and both modalities, our ERP and ERF effects showed a clear baseline of activity before stimulus presentation, and effects during stimulus presentation were well-localized in time, thus speaking to the overall quality of data collected. As noted above, it is important to emphasize that these are preliminary results that will need to be confirmed by further analyses.

Harmonic Complex Sound Stimuli

As predicted, behavioral results for the attentive HCS condition showed that participants reacted significantly faster when identifying large deviant stimuli as compared to intermediate and small deviant stimuli (Figure 2B). This result is in line with analyses of the ERPs, where MMN and P3b components consistently showed the largest and earliest peak amplitudes for large deviant stimuli as compared to intermediate and small deviants (Figure 3, Figure 5). This pattern held true across time windows (100-190 ms and 260-420 ms for MMNs, 70-200 ms and 200-550 ms for P3bs) and across modalities, as similar results were found in the analyses of the ERFs (Figure 4, Figure 6). These findings confirm that the large deviant stimuli were easier to process because they were most different from the standard stimuli (40 Hz difference). However, some differences were also found between modalities: while both the MMN and the P3b amplitudes had a significant main effect of deviance in the later latency bands (260-420 ms for the MMN and 200-550 ms for the P3b), the main effect of deviance was not significant for the MMNm and the P3bm amplitudes. In addition, regarding P3b (70-200 ms) and MMNm (100-190 ms) latencies, large deviants were not associated with the earliest peaks, as would be expected. These results can possibly be explained by the algorithm not selecting the correct values for the intermediate and small deviants that, in contrast with the large deviants, were not associated with clear peaks (Figure 5, Figure 4). Further verifications will be performed to test this hypothesis. Thus, overall, the results for large deviant amplitude and latency align with existing EEG literature, as MMN and P3b amplitude have both been shown to increase and their latencies to decrease as stimulus difficulty decreases (Näätänen, Paavilainen, Rinne, & Alho, 2007; Picton, 1992). Interestingly, while this pattern has, to our knowledge, not been examined in MEG studies, our results indicate that similar fluctuations in amplitude may hold true for MMNm and P3bm components. Thus, these results help validate our protocol, confirming that at the level of pre-attentive and attentive processing as captured by EEG and

MEG recording as well as at the behavioral level, the large deviant stimulus, which differs to the greatest extent from standard deviant stimuli, was the easiest to process.

Another interesting effect regarding HCS MMN and MMNm components for large deviant stimuli was the presence of an early and late peak, captured by the 100-190 ms and 260-400 ms time windows (Figure 3, Figure 4). The presence of these two peaks may have created discrepancies in our main effect of latency results, where we often did not see significant main effects of latency (MMN 100-190 ms, 260-420 ms; MMNm 260-420 ms). This likely occurred because although large deviant stimuli had early MMN and MMNm peaks that intermediate and small deviant stimuli did not have, this early peak was not captured in the late time window, where the other peaks occurred. This will be corrected in the coming weeks by using a longer time window (for example, 100-420 ms) for latency analyses. Additionally, the double peak seen for large deviant stimuli differs from a typical MMN or MMNm response and was not seen for the small or intermediate deviant stimuli (Figure 3, Figure 4). Interestingly, Thiede et al., 2020 recently reported a similar finding, where they saw early (125-170 ms) and late (325-370 ms) MMNm components in response to syllable stimuli where deviant stimuli had differing vowel duration, identity, or frequency. While these stimuli align more with the syllable stimuli used here, we did not see this effect in our syllable conditions. Nevertheless, a late MMN has also been shown to be evoked by tone stimuli with changes in pitch (Schulte-Körne, Deimel, Bartling, & Remschmidt, 2000). The functional significance of the double peak seen for large deviant stimuli remains unclear and should be investigated in future studies. Overall, the presence of early and late MMN and MMNm components is an intriguing phenomenon, and it is interesting to note that here, it is captured similarly by both EEG and MEG recordings.

There were also differences seen when comparing pre-attentive and attentive processing of HCS stimuli. For this paper, the analysis of these differences will be qualitative, but they will be tested through additional statistics in the coming weeks. In general, when comparing the absolute values of peak amplitudes between pre-attentive and attentive conditions, amplitudes were larger in attentive than pre-attentive conditions regardless of the modality (MMN 100-190 ms = 1.09 μV, P3b 200-550 ms = 1.97 μV; MMNm 100-190 ms = 35 fT, P3bm 70-200 ms = 54.9 fT). This indicates that overall, neuronal responses to auditory stimuli were larger when participants were paying attention than when they were not, as has been shown in existing literature (Lakatos et al., 2013). This makes sense when considering that attentive processing mobilizes more cognitive resources, which could lead to great neuronal activity overall. To further investigate the effects of attention in auditory processing, it will also be of interest to compare the differences between the three deviants in the pre-attentive and attentive

conditions. This will be done in future analyses by taking the difference wave of difference waves, for example by subtracting the small deviant curve from the large deviant curve in both the pre-attentive and attentive conditions to determine which type of attention yields a greater difference in neuronal responses.

Syllable Stimuli

For the SYL stimuli, behavioral results showed that reaction times were significantly shorter for the identification of aspiration and pitch deviant stimuli than for voicing deviant stimuli (Figure 5B). These results are mostly in line with the ERP data, where the aspiration deviant often had a larger and earlier peak than voicing and pitch deviants across time windows, type of attention conditions, and modalities. Together, these results can be taken as an indication that aspiration deviant stimuli were more easily recognized and thus were often processed earlier and with larger MMN, MMNm, P3b, and P3bm components than pitch and voicing deviant stimuli. When considered in the context of the French phonetic repertoire, this result can appear contradictory, as neither aspiration nor pitch contrasts exist in French, but voicing contrasts do. This result was thus contrary to our hypothesis that the voicing deviant would be the easiest to recognize and would produce the largest and earliest MMN, MMNm, P3b, and P3bm components, as well as the lowest percent error and the quickest reaction time in behavioral results. However, this pattern of results is possibly linked to the difference in acoustic parameters between the aspiration deviant syllable and the standard syllable being larger than that of the voicing deviant syllable. In a next step, it will be interesting to conduct an acoustic analysis to further test this interpretation. If this were the case, it would indicate that acoustic parameters may be more important than linguistic relevance in determining the ease of identifying sounds.

Some surprising results regarding SYL stimuli came from the pre-attentive ERP and ERF conditions, where MMN and MMNm components were either not localized as expected (Figure 8) or had smaller amplitudes than in pre-attentive HCS conditions (Figure 9). MMNs are known to be larger over frontal and central regions (Näätänen, Pakarinen, Rinne, & Takegata, 2004; Rinne, Alho, Ilmoniemi, Virtanen, & Näätänen, 2000), however our SYL ERPs showed frontal positivities, not negativities, and MMNs were seen at parietal ROIs. For MMNm data, both positivities and negativities were seen, with most activity occuring at central and parietal ROIs. While the positivities do not align with typical MMN patterns in EEG data, it is important to note that in ERF data, previous literature has interpreted components regardless of their polarity, and thus we can likely interpret both positive and negative pre-attentive peaks as MMNm components (Joliot, et al., 2009). However, the localization of

MMNs remains incoherent with the literature, and will be investigated further using topographic maps across time at the individual level.

When comparing across modalities for pre-attentive and attentive SYL results, there were less instances of significant main effects of deviance and significant deviance-by-ROI interactions in MEG data than in EEG data, specifically for the late P3b and P3bm windows. When examining data qualitatively, it appears that this may be due to an inversion in ERF polarity between left and right hemispheres, as well as a general lack of activity along the midline (Figure 9, Figure 11). This pattern is present in HCS ERF results as well (Figure 4, Figure 6), but is absent from ERP results. One potential explanation for this polarity inversion could be that the area along the midline between the two sets of peaks is the source of pre-attentive and attentive processing activity of the different auditory stimuli. The reasoning that the area between an inversion of polarity may be a source location has been used when describing auditory evoked potentials using sEEG and MEG (Godey, Schwartz, de Graaf, Chauvel, & Liégeois-Chauvel, 2001). Regardless of whether this proves true, the opposite polarities on left and right hemispheres likely cancel out near the midline, which would contribute to the lack of activity seen along this region. These hypotheses remain to be tested through further statistical analyses to confirm that the polarity inversion is significant, as well as through source localization to determine the position of a generator, which will be performed in the coming weeks.

Finally, when comparing pre-attentive and attentive results for SYL stimuli, we can see that, as with HCS results, attentive components seem to be larger overall than pre-attentive components, especially when comparing late time windows. For example, for the absolute values of aspiration deviant peak amplitudes, the late MMN peak (140-300 ms) was 0.90 µV, whereas for the P3b component in the later time window (250-500 ms) it was 1.96 µV. Similarly, in MEG, the late MMNm peak (300-450 ms) was 32.0 fT, whereas the P3bm peak in the later time window (100-250 ms) was 45.0 fT. Thus, effects in both the HCS and SYL conditions seem to be larger in attentive than pre-attentive conditions, regardless of the modality. As stated above, this remains to be confirmed using statistical tests on the difference of difference waves in pre-attentive and attentive conditions for each type of deviant stimuli. Another interesting point of contrast comes from the ERP and ERF responses to the pitch deviant in pre-attentive and attentive conditions. In both the MMN and MMNm conditions, the activity corresponding to the pitch deviant seems qualitatively different from the activity associated to the other two deviants, remaining around the baseline level of activity and displaying long-lasting positivities and negativities with no clear peak (Figure 8, Figure 9).

Meanwhile, in the P3b and P3bm conditions, the pitch deviant peaks are more similar to those seen for aspiration and voicing deviants (Figure 10, Figure 11). This may indicate a difference in pitch processing between pre-attentive and attentive conditions at the individual level. If participants were automatically recognizing pitch deviants at different latencies in pre-attentive conditions, this could contribute to the spread-out and long-lasting effects for pitch deviant stimuli. By contrast, in the attentive condition, the identification task may have minimized these differences. Again, this result remains to be confirmed with additional statistical analyses as well as examination of results at the individual level.

Conclusions and Future Directions

Overall, the results presented here address our objectives of comparing the pre-attentive and attentive processing of non-linguistic and linguistic sounds using simultaneous EEG and MEG recordings at the sensor-level. We have begun analysis of our data at the source-level to answer our final questions about how the locations of pre-attentive and attentive processing differ and how EEG and MEG can be used to determine these locations. Through ERP and ERF data, our results have indicated that large deviants, for HCS stimuli, and aspiration deviants, for SYL stimuli, were the easiest to recognize and process on pre-attentive and attentive levels. They also show important similarities between ERP and ERF data, where many of the patterns captured by EEG were also seen in MEG results, especially for HCS stimuli. Finally, our investigations indicate differences between pre-attentive and attentive processing captured mainly by EEG, where attentive processing of auditory stimuli produces components with larger amplitudes overall than pre-attentive processing of the same stimuli. Thus, this study provided a comprehensive look at auditory processing differences across modalities and attention conditions.

I will continue working on this project through the month of June during which we plan to complete the remaining statistical tests at the sensor-level (mainly post hoc analyses) and begin source-level localizations. Once finished, we hope to describe the full scope of our results in a paper to submit for publishing.

Recontextualization

My M2 research internship with Dr. Mireille Besson (MB) and Dr. Valérie Chanoine (VC) served as a continuation of the work that I did during the M1 internship. This meant that I had the time and resources to be involved in each step of our experiment, from establishing the theoretical questions to analyzing and presenting the data we gathered. While the first year of research involved getting familiar with our protocol and analyzing preliminary EEG results,

this year we finished testing all our participants and I dedicated a large portion of my time to learning how to analyze our EEG and MEG data using MNE-Python.

At the beginning of the M2 internship in February, I worked with MB and VC to finish the EEG analysis for the subjects we had tested during my M1 internship. To do this, we used MNE-Python programs that I learned to code under the instruction of VC which allowed us to determine which of our subjects we would be able to keep for the rest of our analyses and how many additional participants we would need to test during the rest of the year to complete our sample size. We also met with the rest of the team involved in the project (Dr. Jean-Michel Badier (JMB) and Khoubeib Kanzari (KK)) at the MEG Center at the Timone Hospital, where I presented the results that we had at that point, and we discussed next steps together. Following this meeting and for the rest of the month of February, I met with VC once a week to continue learning how to program using MNE-Python. With her guidance, I learned how to present our behavioral results as well as our ERP results by region of interest. During this time, I also met regularly with MB, and together we looked at initial ANOVA results on our EEG data.

During these discussions, we determined that we needed to test additional participants to make our group sizes more substantial, both so that our results would be more reliable and for potential publishing in the coming months. Thus, we reserved several days of experiments at the MEG Center, which took place in March. I helped recruit participants and communicated with them regarding the experiment's inclusion criteria. I was present for each of the experiment days, where I worked with Thomas Chehrerian (another M2 student) to run the experiment from beginning to end, with help from JMB and KK when we ran into technical issues. This included setting up MEG, EEG, and stimuli computers and programs, preparing participants for MEG by performing a compatibility test, and for EEG by placing their electrode caps and external electrodes, explaining the tasks to the participants, setting them up in the MEG room, starting EEG and MEG recordings, and monitoring the data gathered throughout the experiment. Because I had begun learning this protocol during my M1 internship, I was very familiar with the procedure at this point and, together with MB, KK, and JMB, I was able to help teach the process to new M1 and L3 interns.

Once we were done testing our additional participants, during the rest of March and into April we performed the same analyses we had done on our EEG data, but this time on the combined EEG and MEG data. I worked with VC to learn how to develop scripts that would read combined EEG and MEG files and perform initial quality tests on the data, which allowed us to examine our data at the individual participant level. I then spent several weeks working both with MB and independently to use MNE-Python to perform these quality tests, which

allowed us to determine the quality of recordings for each EEG and MEG captor and for each participant, and to decide whether there were certain captors we wanted to eliminate due to high levels of noise across trials. Once this step was complete, I worked with MB and VC to finalize ERP and ERF results and run statistical analyses on the data. In parallel, I spent time writing my thesis, which I structured such that it could be transformed into an article once our EEG and MEG results at the sensor and source levels were finalized.

When I came to Marseille for the Cognitive Science Master's after studying biology and doing neurobiology research during my undergraduate degree, my main goal was to be exposed to cognitive neuroscience research, an area that I had not seen much of previously. This internship allowed me to meet that goal, as I became familiar with every stage of running a cognitive neuroscience study, including recruiting and working with human participants, something I had never done before. I also learned how to record and interpret both EEG and MEG signals, and how to analyze these data using Python, a tool I had never used before and that I know will be extremely useful in all my future endeavors. Beyond the technical skills I learned that will support me going forward, this internship also taught me valuable lessons about collaboration in research. Our study spanned several different fields from EEG and MEG experimentation to programming and data science, which meant that we were constantly communicating with experts from these different fields and coordinating between different groups of people. Thus, I was able to work with and learn from these different experts in different settings: with MB I learned how to perform EEG experiments, read and interpret EEG results, and how to consider questions from a critical, scientific perspective, with JMB and KK I learned how to use MEG machinery and troubleshoot any technical issues that arose from stimuli presentation, and with VC I learned how to write Python code and analyze combined EEG and MEG data. I also practiced presenting our data and experienced being a part of big-picture discussions regarding our research goals when we would all come together to discuss where we were in our study. My next academic goal is to complete a PhD in neuroscience, and I know that the skills I learned during this internship will be crucial in helping me reach this goal and in allowing me to continue a career in neuroscience research.

References

Alho, K., Winkler, I., Escera, C., Huotilainen, M., Virtanen, J., Jääskeläinen, I. P., . . . Ilmoniemi, R. J. (2001). Processing of novel sounds and frequency changes in the human auditory cortex: Magnetoencephalographic recordings. *Psychophysiology, 35*(2), 211-224.

Baillet, S. (2011). Electromagnetic brain mapping using MEG and EEG. In *The Oxford handbook of social neuroscience* (pp. 97-133). Oxford University Press.

Colombet, B., Woodman, M., Badier, J., & Bénar, C. G. (2015). AnyWave: a cross-platform and modular software for visualizing and processing electrophysiological signals. *Journal of neuroscience methods, 242*, 118-126.

Dien, J., Spencer, K. M., & Donchin, E. (2003). Localization of the even-related potential novelty response as defined by principal components analysis. *Cognitive Brain Research, 17*, 637-650.

Donchin, E. (1981). Surprise!… surprise? *Psychophysiology, 18*(5), 493-513.

Fitzgerald, K., & Todd, J. (2020). Making sense of mismatch negativity. *Frontiers in Psychiatry, 11*, 468.

Frey, A., Barbaroux, M., Dittinger, E., & Besson, M. (2022). Effects of Psychoacoustic Training on the Pre-Attentive Processing of Harmonic Sounds and Syllables. *Journal of Speech, Language, and Hearing Research*, 1-13.

Fujioka, T., Trainor, L. J., Ross, B., Kakigi, R., & Pantev, C. (2004). Musical training enhances automatic encoding of melodic contour and interval structure. *Journal of cognitive neuroscience, 16*(6), 1010-1021.

Godey, B., Schwartz, D., de Graaf, J. B., Chauvel, P., & Liégeois-Chauvel, C. (2001). Neuromagnetic source localization of auditory evoked fields and intracerebral evoked potentials: a comparison of data in the same patients. *Clinical Neurophysiology, 112*, 1850-1859.

Gordon, E., Slogget, G., Harvay, I., Kraiuhin, C., Pennie, C., Yiannikas, C., & Meares, R. (1987). Magnetoencephalography: locating the source of P300 via magnetic field recording. *Clinical and Experimental Neurology, 23*, 101-110.

Gramfort, A., Luessi, M., Larson, E., Engemann, D. A., Strohmeier, D., Brodbeck, C., . . . Hämäläinen, M. S. (2013). MEG and EEG data analysis with MNE-Python. *Frontiers in Neuroscience, 7*(267), 1-13.

Ha, K. S., Youn, T., Kong, S. W., Park, H.-J., Ha, T. H., Kim, M. S., & Kwon, J. S. (2003). Optimized Individual Mismatch Negativity Source Localization Using a Realistic Head Model and the Talairach Coordinate System. *Brain Topography, 15*, 233-238.

Hari, R. (1990). Magnetic evoked fields of the human brain: basic principles and applications. *Electroencephalography and Clinical Neurophysiology, 41*, 3-12.

He, B., Lian, J., Spencer, K. M., Dien, J., & Donchin, E. (2001). A cortical potential imaging analysis of the P300 and novelty P3 components. *Human Brain Mapping*, 120-130.

Huotilainen, M., Winkler, I., Alho, K., Escera, C., Virtanen, J., Ilmoniemi, R. J., . . . Näätänen, R. (1998). Combined mapping of human auditory EEG and MEG responses. *Electroencephalography and clinical Neurophysiology*, 370-379.

Joliot, M., Leroux, G., Dubal, S., Tzourio-Mazoyer, N., Houdé, O., Mazoyer, B., & Petit, L. (2009). Cognitive inhibition of number/length interference in a Piaget-like task: Evidence by combining ERP and MEG. *Clinical Neurophysiology, 120*, 1501-1513.

Korostenskaja, M., Kičić, D., & Kähkönen, S. (2008). The effect of methylphenidate on auditory information processing in healthy volunteers: a combined EEG/MEG study. *Psychopharmacology*, 475-486.

Lakatos, P., Musacchia, G., O'Connel, M. N., Falchier, A. Y., Javitt, D. C., & Schroeder, E. C. (2013). The Spectrotemporal Filter Mechanism of Auditory Selective Attention. *Neuron, 77*, 750-761.

Larson, E., Gramfort, A., Engemann, D. A., Leppakangas, J., Brodbeck, C., Jas, M., . . . Brunner. (2023). *MNE-Python (v1.3.1)*. Retrieved from Zenodo: https://doi.org/10.5281/zenodo.7671973

Lecaignard, F., Bertrand, O., Caclin, A., & Mattout, J. (2021). Empirical Bayes evaluation of fused EEG-MEG source reconstruction: Application to auditory mismatch evoked responses. *NeuroImage, 226*.

Linden, D. E. (2005). The P300: Where in the Brain Is It Produced and What Does It Tell Us? *The Neuroscientist, 11*(6), 563-576.

Maassen, B., Groenen, P., Crul, T., Assman-Hulsmans, C., & Gabreëls, F. (2001). Identification and discrimination of voicing and place-of-articulation in developmental dyslexia. *Clinical Linguistics & Phonetics, 15*(4), 319-339.

Mäkelä, J. P., Hämäläinen, M., Hari, R., & McEvoy, L. (1994). Whole-head mapping of middle-latency auditory evoked magnetic fields. *Electroencephalography and Clinical Neurophysiology, 95*, 405-414.

Näätänen, R. (1992). Attention and brain function. *Psychology Press*.

Näätänen, R., Gaillard, A. W., & Mäntysalo, S. (1978). Early selective-attention effect on evoked potential reinterpreted. *Acta psychologica*, 313-329.

Näätänen, R., Paavilainen, P., Rinne, T., & Alho, K. (2007). The mismatch negativity (MMN) in basic research of central auditory processing: a review. *Clinical neurophysiology, 118*(12), 2544-2590.

Näätänen, R., Pakarinen, S., Rinne, T., & Takegata, R. (2004). The mismatch negativity (MMN): towards the optimal paradigm. *Clinical neurophysiology*, 140-144.

Nakasato, N., Fujita, S., Seki, K., Kawamura, T., Matani, A., Tamura, I., & Fujiwara, S. (1994). Functional localization of bilateral auditory cortices using an MRI-linked whole head magnetoencephalography (MEG) system. *Electroencephalography and Clinical Neurophysiology, 94*, 183-190.

Nishitani, N., Nagamine, T., Fujiwara, N., Yazawa, S., & Shibasaki, H. (1998). Cortical-hippocampal auditory processing identified by magnetoencephalography. *Journal of Cognitive Neuroscience, 10*, 231-247.

Osorio, S., Irani, M., Herrada, J., & Aboitiz, F. (2022). Neural responses to sensory novelty with and without conscious access. *NeuroImage, 262*.

Pakarinen, S., Takegata, R., Rinne, T., Huotilainen, M., & Näätänen, R. (2007). Measurement of extensive auditory discrimination profiles using the mismatch negativity (MMN) of the auditory event-related potential (ERP). *Clinical Neurophysiology, 118*, 177-185.

Pantev, C., Bertrand, O., Eulitz, C., Verkindt, C., Hapson, S., Schuierer, G., & Elbert, T. (1995). Specific tonotopic organizations of different areas of the human auditory cortex revealed by simultaneous magnetic and electric recordings. *Electroencephalography and Clinical Neurophysiology, 94*, 26-40.

Picton, T. W. (1992). The P300 wave of the human event-related potential. *Journal of clinical neurophysiology, 9*(4), 456-479.

Polich, J. (2003). Theoretical overview of P3a and P3b. *Detection of change*, 83-98.

Polich, J. (2007). Updating P300: an integrative theory of P3a and P3b. *Clinical neurophysiology, 118*(10), 2128-2148.

Puce, A., & Hämäläinen, M. S. (2017). A Review of Issues Related to Data Acquisition and Analysis in EEG/MEG Studies . *Brain Sci.*

Reite, M., Sheeder, J., Teale, P., Richardson, D., Adams, M., & Simon, J. (1994). MEG based brain laterality: sex differences in normal adults. *Neuropsychologia, 33*, 1607-1616.

Rinne, T., Alho, K., Ilmoniemi, R. J., Virtanen, J., & Näätänen, R. (2000). Separate time behaviors of the temporal and frontal mismatch negativity sources. *Neuroimage, 12*(1), 14-19.

Rogers, R. L. (1991). Localization of the P3 sources using magnetoencephalography and magnetic resonance imaging. *Electroencephalography and Clinical Neurophysiology, 79*, 308-321.

Rogers, R. L., Papanicolaou, A. C., Baumann, S. B., Saydjari, C., & Eisenberg, H. M. (1990). Neuromagnetic evidence of a dynamic excitation pat- tern generating the N100 auditory response. *Electroencephalography and Clinical Neurophysiology, 77*, 237-240.

Schulte-Körne, G., Deimel, W., Bartling, J., & Remschmidt, H. (2000). Speech perception deficit in dyslexic adults as measured by mismatch negativity žMMN/. *International Journal of Psychophysiology, 40*, 77-87.

Seabold, S., & Perktold, J. (2010). Statsmodels: Econometric and statistical modeling with python. *Proceedings of the 9th Python in Science Conference*.

Sharon, D., Hämäläinen, M. S., Tootell, R. B., Halgren, E., & Belliveau, W. J. (2007). The advantage of combining MEG and EEG: comparison to fMRI in focally-stimulated visual cortex. *Neuroimage, 36*(4), 1225-1235.

Shestakova, A., Brattico, E., Huotilainen, M., Galunov, V., Soloviev, A., Sams, M., . . . Näätänen, R. (2002). Abstract phoneme representations in the left temporal cortex: magnetic mismatch negativity study. *Neuroreport, 13*(14), 1813-1816.

Siedenberg, R., Goodin, D. S., Aminoff, M. J., Rowley, H. A., & Roberts, T. P. (1996). Comparison of late components in simultaneously recorded event-related electrical potentials and event-related magnetic fields. *Electroencephalography and clinical Neurophysiology, 99*(2), 191-197.

Sugg, M. J., & Polich, J. (1995). P300 from auditory stimuli: intensity and frequency effects. *Biological psychology, 41*(3), 255-269.

Takahashi, H., Rissling, A. J., Pascual-Marqui, R., Kirihara, K., Pela, M., Sprock, J., . . . Light, G. A. (2012). Neural substrates of normal and impaired preattentive sensory discrimination in large cohorts of nonpsychiatric subjects and schizophrenia patients as indexed by MMN and P3a change detection responses. *NeuroImage*, 594-603.

Tarkka, I. M., Stokic, D. S., Basile, L. F., & Papanicolaou, A. C. (1995). Electric source localization of the auditory P300 agrees with magnetic source localization. *Electroencephalography and Clinical Neurophysiology, 96*, 538-545.

Thiede, A., Parkkonen, L., Virtala, P., Laasonen, M., Mäkelä, J. P., & Kujala, T. (2020). Neuromagnetic speech discrimination responses are associated with reading-related skills in dyslexic and typical readers. *Heliyon*.

Winterer, G., Mulert, C., Mientus, S., Gallinat, J., Schlattmann, P., Dorn, H., & Herrmann, W. M. (2001). P300 and LORETA: Comparison of Normal Subjects and Schizophrenic Patients. *Brain Topography, 13*, 299-313.

Appendix A

Appendix B

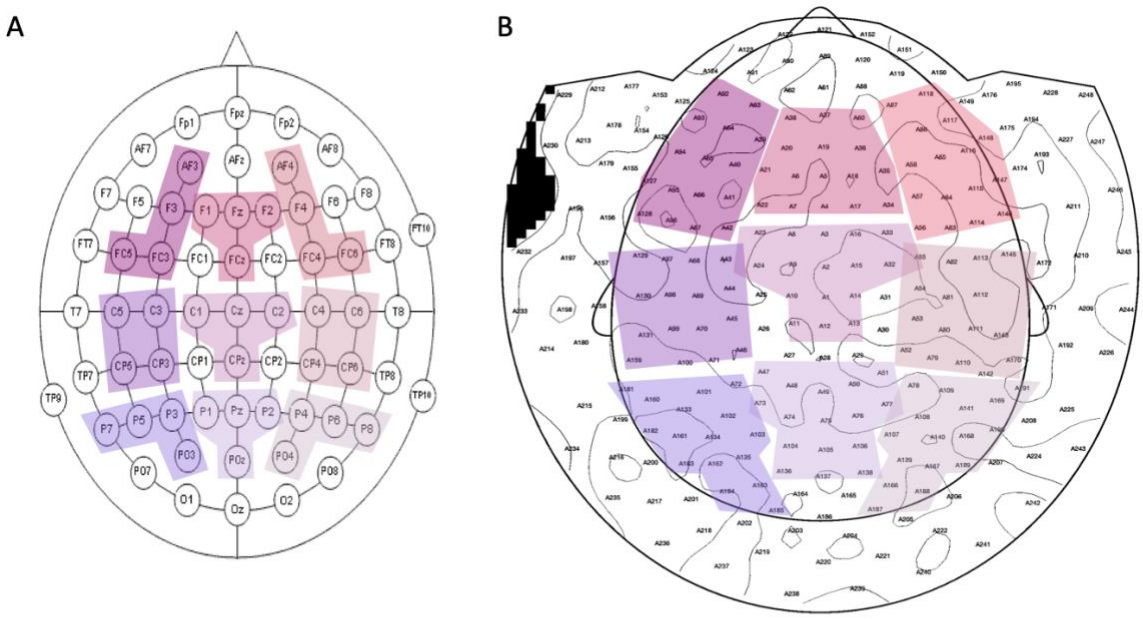

Appendix B. Regions of interest (ROIs) used for EEG and MEG analyses. For EEG analysis (A), ROIs were drawn on a 64-electrode cap template with 10-20 system naming. Captors not included in ROIs were those with consistently high levels of noise across recordings. Each ROI contains 4 electrodes. For MEG analysis (B), ROIs were drawn on a 248 magnometer system template, and were made to match the positions of EEG ROIs as closely as possible. Each ROI contains 16 sensors. In both cases, the following 9 ROIs were used for analyses: Frontal Left, Central Left, Parietal Left, Frontal Midline, Central Midline, Parietal Midline, Frontal Right, Central Right, Parietal Right.